Open Access

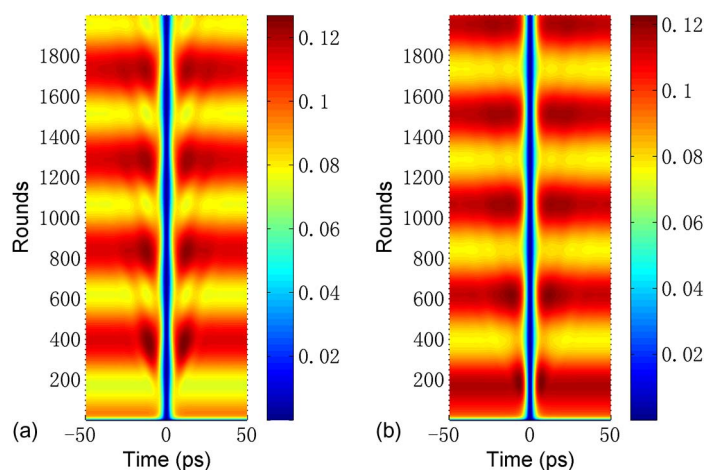# Formation and Energy Exchange of Vector Dark Solitons in Fiber Lasers

Jun Guo
Yuanjiang Xiang
Xiaoyu Dai
Han Zhang
Shuangchun Wen

Formation and Energy Exchange of Vector Dark Solitons in Fiber Lasers

Jun Guo,[1] **Yuanjiang Xiang,**[2] **Xiaoyu Dai,**[2]
Han Zhang,[1,2] **and Shuangchun Wen**[1]

[1]Laboratory for Micro-/Nano-Optoelectronic Devices of Ministry of Education,
School of Physics and Electronics, Hunan University, Changsha 410082, China
[2]SZU-NUS Collaborative Innovation Center for Optoelectronic Science and Technology,
Key Laboratory of Optoelectronic Devices and Systems of Ministry of Education and Guangdong
Province, College of Optoelectronic Engineering, Shenzhen University, Shenzhen 518060, China

Abstract: The mutual energy-exchange interactions in two orthogonally polarized components of vector dark soliton, which is automatically formed in a normal-dispersion fiber laser cavity in the presence of reverse saturable absorption, and dissipative cavity effects, had been theoretically and numerically investigated. Under specific cavity parameters, a vector dark soliton with periodic coherent energy exchange could be formed and well described by a semianalytic method. The multiple vector dark solitons with energy exchange were also demonstrated by combining gain bandwidth and a reverse saturable absorption effect.

Index Terms: Optical solitons, fiber lasers, fiber nonlinear optics.

1. Introduction

Soliton formation in nonlinear optics is an attractive topic that has been extensively investigated [1]. The main nonlinear equation governing the pulse evolution is the famous nonlinear Schrodinger equation (NLSE) which, depending on the sign of the group-velocity dispersion, has two distinct types of solutions: bright or dark solitons. Optical solitons could be automatically formed due to the natural balance between the dispersion and the nonlinear optical Kerr effect. In particular, dark solitons, which are intensity dips embedded in a CW background, are formed in the normal dispersion.

Dark solitons have attracted considerable attention, and been studied in diverse branches of physics, especially in the fields of nonlinear optics [2] and Bose-Einstein condensates (BECs) [3]. In BECs dark solitons, also called "kink-states," exists because of repulsive interactions [4], [5], correspond to the case of normal optical dispersion in optical fibers. In the context of BECs theoretical studies on dark solitons started as early as 1971 [6]. Thereafter, the first prediction of dark solitons in nonlinear optical fibers at the normal dispersion regime was completed [7] and then extensively studied [1], [2]. There also exist many experimental results on dark solitons

in BECs [4], single mode fibers (SMFs) [8], and in mode-locked fiber lasers [9]. It was shown that dark solitons are more robust against external noise or perturbations. Owing to the relatively weak interaction among adjacent dark solitons, they are suggested to have the feasibility of applications in optical communications [10].

Scalar NLSE can be extended to the coupled NLSEs considering different polarization or optical modes in nonlinear optics [2] or two component condensates in BECs [3]. Thus vector solitons emerge with diverse dynamics. Vector bright solitons have been extensively studied in both theoretical and experimental aspects [11]–[17]. Various dynamics have been studied both in nonlinear optics and BECs [18], [19], for example, energy exchange, which is one important feature of vector bright solitons, is usually due to four-wave mixing [16] or collision [17] in nonlinear optics. In BECs, matter wave solitons interact basically in the same way as optical solitons [18].

While scalar dark solitons and vector bright solitons has been studied extensively, vector dark solitons described by coupled NLSE was much less addressed. The interaction of two optical modes had been studied and vector dark solitons were firstly predicted by Kivshar *et al.* [20]. Thereafter, vector dark solitons in isotropic Kerr media with different polarization were predicted by Sheppard *et al.* [21], and Seve *et al.* presented an experimental observation of vector dark-soliton pulse trains in optical fibers [22]. Vector dark solitons were also studied in two-component BECs [23], [24] and presented novel and fundamentally different scenarios for single-component ones.

The previous studies on vector dark solitons in nonlinear optics mainly focus on the propagation in optical fibers or isotropic Kerr media. In a fiber laser, besides the mutual balance between the optical nonlinearity and fiber dispersion, cavity gain effect and linear or nonlinear loss will also play a central role in determining the soliton features, leading to richer dynamics than that of soliton formed in optical fiber. However, despite of the existence of laser gain and cavity output, the essential dynamics of the solitons are still governed by the NLSE [25], [26]. Thus, vector dark solitons are expected to exist also in fiber lasers, but other nonlinear optical effects such as saturable absorber or filter should also be considered.

The purpose of this work is to extend the scalar dark solitons in fiber lasers to vector dark solitons, and investigate their mutual interactions and the corresponding propagation properties. Due to extra parameters introduced by the cavity, such as birefringence, gain parameter and reverse saturable absorption (RSA), rich dynamics of vector dark solitons can be expected. In the meanwhile, the governing equation of fiber lasers is extended to the coupled NLSEs [27], the results obtained might be instructive for vector dark solitons in other physics, like BEC physics.

We also propose a semi-analytic method, though full numerical simulations provide good agreement with experiments, they are usually time-consuming, and make exploration of large parameter space difficult. Especially in fiber lasers, thousands of round trips calculations are usually needed to get a stable solution. This kind of approximate technique can usually simplify the governing nonlinear partial differential equation into a set of coupled ordinary differential equations [28]–[31] which can be solved much more quickly using standard techniques, such as fourth-order Runge-Kutta method, than full numerical simulation.

2. Simulations and Semi-Analytic Method

The light circulation in a unidirectional fiber ring cavity is governed by the following extended coupled NLSE [27]:

$$i\frac{\partial u_\pm}{\partial z} - \frac{\beta_2}{2}\frac{\partial^2 u_\pm}{\partial t^2} + \gamma\left(|u_\pm|^2 + \frac{2}{3}|u_\mp|^2\right)u_\pm + \frac{1}{3}\gamma u_\pm^* u_\mp^2 \pm \kappa u_\pm - i\frac{g}{2}u_\pm - i\frac{g}{2\Omega_g^2}\frac{\partial^2 u_\pm}{\partial t^2} + il|u_\pm|^2 u = 0 \quad (1)$$

where $u_\pm$ is the slowly varying amplitude of the two orthogonal linearly polarized eigen-modes of the cavity, β_2 is the cavity dispersion parameter, γ is the nonlinearity of the fiber, κ is the
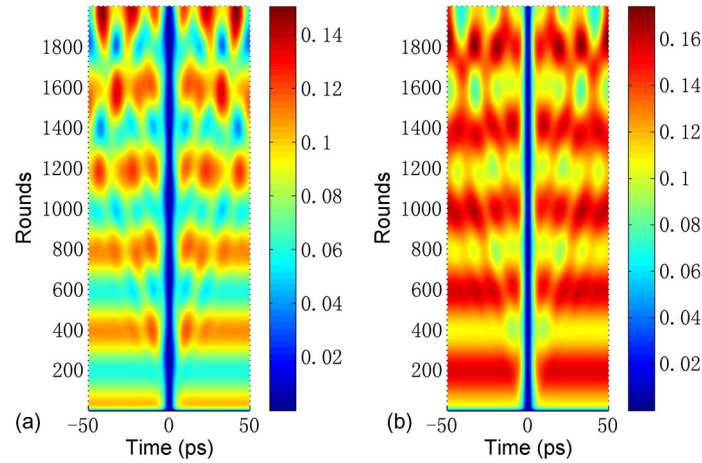
Fig. 1. Complete evolution of the initial profile of two polarized states (a) u_+ and (b) u_- for $E_s = 0.33$ pJ, $\kappa = -0.2$ km^{-1}, and $l = 0$ km^{-1}.

birefringence, g is the effective laser gain coefficient, and Ω_g is the effective bandwidth of the laser gain. The gain saturation of the laser is described by

$$g = \frac{g_0}{1 + \int \left(|u_+|^2 + |u_-|^2 \right) dt / E_s} \tag{2}$$

where g_0 is a small signal gain and E_s is the saturation energy. The last term of (1) represents the RSA if l is positive. To get RSA in real fiber lasers, the most common method is the nonlinear polarization rotation method, and fiber lasers using this method can be reduced to complex Ginzburg–Landau equation like (1) [32]. In the simulations, we considered a unidirectional ring fiber of which averaged cavity dispersion parameter is $\beta_2 = 6$ ps^2/km, and $\gamma = 3$ W^{-1}km^{-1}. The gain bandwidth is chosen to be 40 nm. The cavity length is set to be 17 m. The small signal gain is 400 km^{-1} and output loss is 10%. The initial condition is set to be a set of arbitrary small black pulses of tanh($\bullet$) profile with arbitrary width. The standard fourth-order Runge-Kutta algorithm was used to numerically solve (1). In our simulations a possibly long simulation window of 100 ps was used and the symmetric boundary technique was adopted.

In Fig. 1, we first show a simulation result without RSA to explain why we should consider this extra effect in the flowing work. The initial input is assumed by a black pulse and the corresponding $E_s = 0.33$ pJ, $\kappa = -0.2$ km^{-1}, and $l = 0$ km^{-1}. As can be seen, without RSA tanh($\bullet$) form initial dark pulses with arbitrary intensity and width will be amplified quickly until the gain is saturate. In Fig. 1, the amplification finishes quickly after only about 20 round trips propagation and the gain is saturate. For most the cases, the final background intensity of dark pulses will be larger than that needed for fundamental dark solitons, then the dark pulses will split like high-order dark solitons in optical fibers and generate lots of symmetrical gray pulses near the central black solitons [1], [2]. On the other hand due to the background fluctuation new gray pulses will be generated constantly. The generated gray pulses can be seen clearly in Fig. 1 after more than 200 round trips propagation. Due to these gray pulses the background will be distorted and hardly analyzed. To avoid these gray pulses, one simple way is to modify the initial dark pulse's width to make it corresponds to the final background intensity when gain is saturate, then vector fundamental black solitons will be formed. However, modifying the initial condition of simulation cannot avoid new gray pulses generated due to background fluctuation, and more importantly, it is not physically meaningful; in real fiber lasers, initial pulses with arbitrary intensity and width could coexist, so we should think about another approach to make the generated gray pulses vanish. Like automatically formation of bright solitons in mode-locked
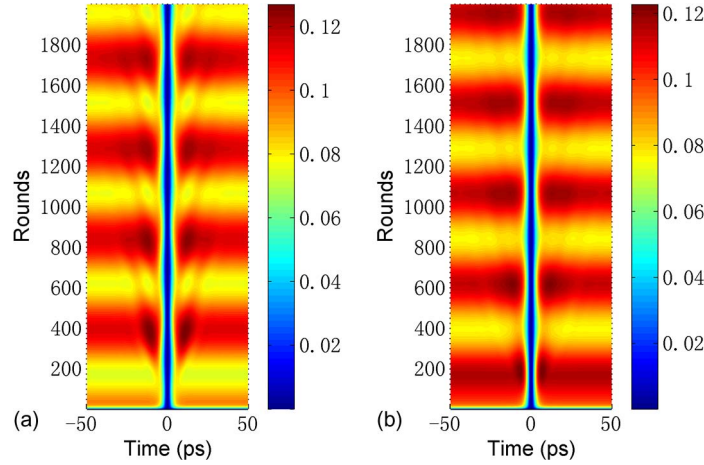
Fig. 2. Complete evolution of the initial profile of two polarized states (a) u_+ and (b) u_- for $E_s = 0.33$ pJ, $\kappa = -0.2$ km^{-1}, and $l = 1$ km^{-1}.

fiber lasers with saturable absorption and anomalous dispersion cavity [27], RSA was also considered helpful in dark soliton formation in fiber lasers with normal dispersion cavity [9], [25]. In our following work, we find that by including RSA effect those gray pulses can be vanished and the soliton profile will be clear and analyzable.

Fig. 2 shows a typical simulation result with RSA involved, where the corresponding $E_s = 0.33$ pJ, $\kappa = -0.2$ km^{-1}, and $l = 1$ km^{-1}. We can see that by including RSA most gray pulses are successfully vanished before they distort the background. As a result each polarized state remain as tanh($\bullet$) profile during their propagation, while both the background and width varies periodically. Due to the period change of background and width, a small portion of dispersive waves will be emitted together with the background wave, while they have no influence on the solitons, and can be reduced by decreasing the averaged cavity dispersion. The period evolution of u_+ is just opposite to u_-, which indicates the existence of periodic energy exchange between these two orthogonally polarized states. By comparing Figs. 1 and 2, we can say in fiber lasers, the role of RSA is very important, it will suppress the existence of any gray pulses. Without RSA, all the gray pulses will survive and collide with each other and also with the black solitons. Then the evolution of solitons will be too complex to be observed and analyzed. We also stress that due to the existence of RSA, solitons in our simulations are all vector black solitons, and vector gray solitons cannot exist.

To further understand results obtained above, using the method described in [25] and extending it to the vector case, we determine the evolution of the background wave in the framework of (1). We assume that

$$u_+^\infty(z) = u_\infty(z)\exp(i\theta(z)), \qquad u_-^\infty(z) = v_\infty(z)\exp(i\phi(z)). \tag{3}$$

Substituting (3) into (1), we get a set of differential equations

$$\frac{\partial u_\infty}{\partial z} = \frac{g}{2}u_\infty - \frac{1}{3}\gamma u_\infty v_\infty^2 \sin(-2\theta + 2\phi) - lu_\infty^3$$

$$\frac{\partial \theta}{\partial z} = \gamma\left(u_\infty^2 + \frac{2}{3}v_\infty^2\right) + \frac{1}{3}\gamma v_\infty^2 \cos(-2\theta + 2\phi) + \kappa$$

$$\frac{\partial v_\infty}{\partial z} = \frac{g}{2}v_\infty - \frac{1}{3}\gamma v_\infty u_\infty^2 \sin(2\theta - 2\phi) - lv_\infty^3$$

$$\frac{\partial \phi}{\partial z} = \gamma\left(v_\infty^2 + \frac{2}{3}u_\infty^2\right) + \frac{1}{3}\gamma u_\infty^2 \cos(2\theta - 2\phi) - \kappa. \tag{4}$$
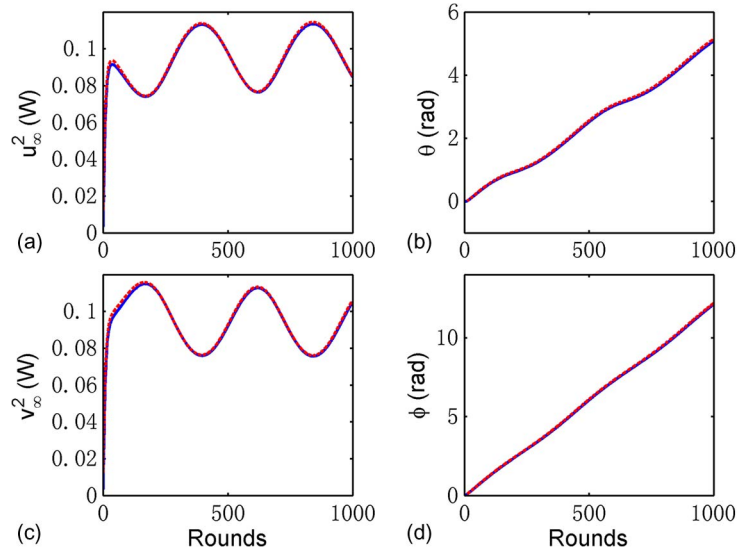
Fig. 3. Semi-analytic results by solving (4) (blue solid lines) and full numerical simulations by solving (1) (red dashed lines) using the same parameters as Fig. 2.

Assuming that during the propagation, both the polarized state remain as black solitons, i.e., $|u_\pm| = |u_\pm^\infty|\tanh(|u_\pm^\infty|t)$. We stress that this assumption is particularly important in the following discussion, if this assumption is proved to be reasonable by comparing semi-analytic and full numerical simulation results, it is enough to discuss the background evolution alone, because according to the assumption, soliton width corresponds to its background intensity. This assumption is also the main difference compared with those methods where more soliton parameters vary during solitons' propagation [28]–[31]. And we also assume that calculation window T_0 is sufficient large, in fact in our numerical simulation a relatively large calculation window is selected, then we get

$$g \approx \frac{g_0}{1 + \left(u_\infty^2 T_0 - 2u_\infty + v_\infty^2 T_0 - 2v_\infty\right)/E_s}. \qquad (5)$$

Note that by (5), the assumed soliton parameters will affect the laser's gain parameter and the soliton parameters will be modified by the gain parameter in return. We can then solve (4) using the fourth-order Runge-Kutta method, which is much faster than complete simulation of (1). The results obtained by this semi-analytic method are shown in Fig. 3. We also compared the semi-analytic results (blue solid lines) with the full numerical simulation of (1) (red dashed lines), the results show good agreement, confirming the accuracy of our semi-analytic method and indicating that during the propagation both polarization remain as fundamental black solitons whose width is determined by the background amplitude. The good agreement between two methods is owe to the effect of RSA, without RSA the semi-analysis method will certainly fail to describe a complex propagation like in Fig. 1.

Using the semi-analytic method, we are able to study the influence of vast cavity parameters on the background evolution much more quickly. In Fig. 4, we show the evolution period of the background with different values of birefringence. It is shown that with larger values of birefringence the evolution period of the background decreases, which means the energy exchange between two polarized states is faster. We also studied other parameters like E_s and I, while they hardly influence the evolution period, only the amplitude of two polarized state was changed. The influence of birefringence on energy exchange period can be easily understood that with larger birefringence, the polarization beat length between two dark solitons will be reduced, and then, the energy exchange between two polarizations will be faster. Moreover if we set κ to be zero, no birefringence is introduced, the period evolution of background will disappear. And
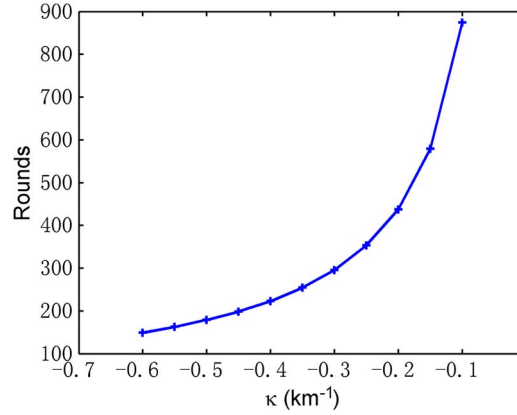
Fig. 4. Evolution period of the background with different values of birefringence.
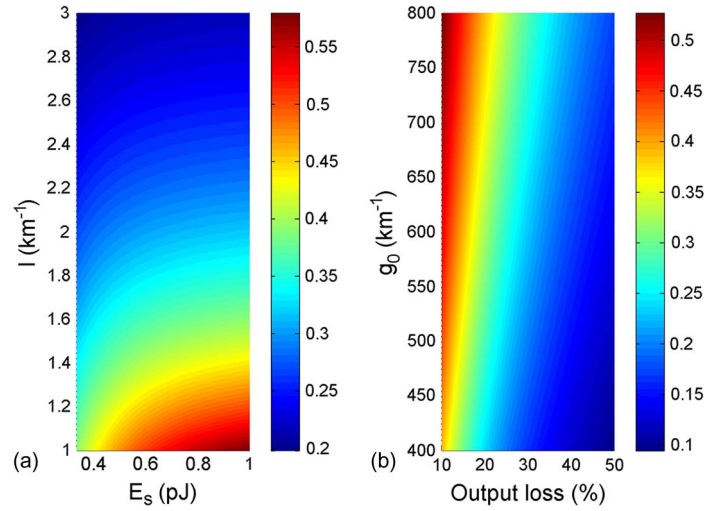

Fig. 5. Contour plot of modulation depth depending on (a) varying values of E_s and l with $g_0 = 400$ km^{-1}, and output loss is 10%; (b) varying values of g_0 and output loss with $E_s = 0.33$ pJ and $l = 1$ km^{-1}. For both cases, $\kappa = -0.2$ km^{-1}.

further if we include the birefringence while dismiss the coherent four wave mixing (FWM) term in (1), which also indicates cases when birefringence has a very large value, the energy exchange will also stop. When energy exchange stops, both two polarizations evolve similarly and keep as fundamental black soliton profile.

We then also define the modulation depth of the period background evolution as

$$M = 2\big(\max\big(u_\infty^2(z)\big) - \min\big(u_\infty^2(z)\big)\big)/\big(\max\big(u_\infty^2(z)\big) + \min\big(u_\infty^2(z)\big)\big) \qquad (6)$$

where max($\bullet$) and min($\bullet$) means the maximum and minimum values of the background amplitude during its period evolution. The defined modulation depth in (6) describes the proportion of energy exchange between two dark solitons, larger M indicates that more proportion of energy is exchanged between two polarizations. We then show the contour plot of modulation depth, depending on varying values of E_s, l in Fig. 5(a) and output loss g_0 in Fig. 5(b). We have calculated with 30×30 points and using interpolation method to plot Fig. 5. As can be seen, the modulation depth increases with increasing values of E_s or decreasing l. Similar results are obtained by varying small signal gain g_0 and output loss, where the modulation depth increases with increasing values of g_0 or decreasing output loss. The above results indicate that when
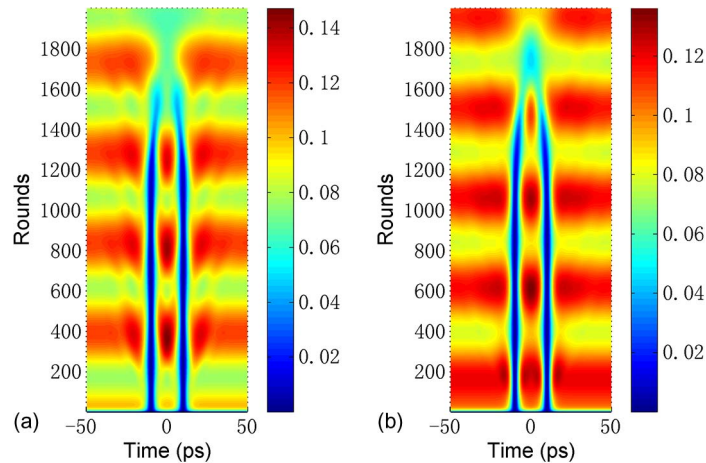
Fig. 6. Two dark soliton evolution for (a) u_+ and (b) u_- using the same cavity parameters as Fig. 2.

vector dark solitons experience larger gain effect or smaller loss, the two polarized state will exchange more proportion of energy periodically.

Finally, we studied the evolution of multiple vector dark solitons, and interaction between two adjacent solitons is also an interesting phenomenon. For adjacent bright solitons, due to their relative phase different, two bright solitons may attract each other if they are in-phase or repel each other if they are out-phase [33]. While for adjacent dark solitons, phase between dark solitons is fixed as they are formed on the same background wave and they are believed to always repel [34]. After our calculations, we found that the RSA will make the dark solitons attract each other. In our simulations the initial condition is set to be two symmetric black pulses for both two polarized state. A typical full numerical simulation of (1) is shown in Fig. 6 using the same parameters as Fig. 2. The background is also evolving periodically, while the adjacent dark solitons collide with each other after more than 1400 rounds propagation, unfortunately all the dark solitons are vanished after collision. After careful observation of the attraction, we found that when two adjacent black solitons are approaching, their darkness will reduce slightly, and this darkness reduction is caused by collision with dispersive waves emitted by the other dark soliton. This kind of dispersive waves is unavoidable due to fluctuation of background waves and arbitrary initial pulse width, and can propagate for more than 400 round trips, as shown in Fig. 2. We can only avoid collision between solitons and dispersive waves by increasing two initial pulses' separation, which is physically meaningless due to arbitrary pulse distributions in real fiber lasers. Meanwhile RSA is sensitive to the reduction of darkness and this is also why RSA can suppress those gray pulses with small darkness. So long as the darkness of black solitons reduces, they start to vanish like those gray pulses under effect of RSA. This is why in Fig. 6 adjacent black solitons start to vanish before they collide, and vanish much more quickly after collision. The attraction is weaker if we reduce the RSA, and the adjacent dark solitons will propagate more round trips before they collide.

By decreasing separation of adjacent dark solitons, we can increase the repelling effect, however the interaction of dark solitons is weak compared to bright solitons, to compensate the attraction adjacent dark solitons should be closely placed, then the same problem appear as the RSA will vanish both the solitons. To get multiple vector dark solitons we should find another effect to compensate the RSA caused attraction, then we found that larger bandwidth effect, i.e., smaller gain bandwidth in (1) fulfill this requirement. In Fig. 7, we show the simulation results with smaller RSA and smaller gain bandwidth to make them balanced. The two adjacent dark solitons can then evolve independently and no collision happens for both two polarized state. And on the other hand, the evolution period of background is hardly affected by the varied parameters comparing to Fig. 2.
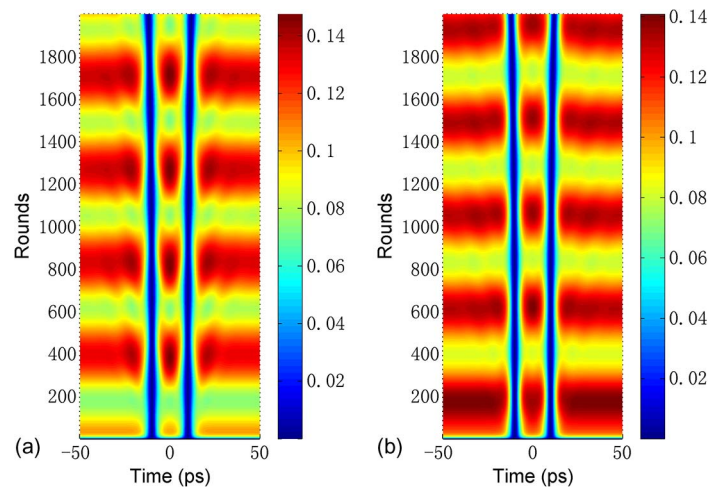
Fig. 7. Two dark soliton evolution for (a) u_+ and (b) u_- with smaller $l = 0.5$ km^{-1} and smaller gain bandwidth $\Omega_g = 20$ nm; the other parameters are the same as Fig. 2.

Based on our calculations, RSA has negative effects on adjacent dark soliton interaction and will cause their collision and vanishing; it seemed not possible to get a stable bound state though balance of RSA caused attraction and intrinsic repelling. Maybe balance between RSA and gain bandwidth will generate a stable bound state, however this also need a large number of numerical simulations, and is out of scope of the present work which mainly discuss vector dark soliton formation. We may prepare another work and discuss the scalar dark soliton interaction in fiber lasers instead.

3. Conclusion

In conclusion, we have studied the generation of vector dark solitons in fiber lasers with RSA numerically and further uncovered the corresponding evolution dynamic by a semi-analytic method. A good agreement between full numerical simulations and the semi-analytic method not only confirmed the accuracy of our method but also indicated that during the propagation both polarizations remain as fundamental black solitons. It is shown that the periodic energy exchange is induced by cavity birefringence and FWM, and the modulation depth is determined by the cavity dissipation parameters. The attraction between multiple dark solitons was found to be induced by RSA and can be balanced by smaller gain bandwidth so that multiple vector dark solitons with periodic energy exchange can be generated. This work might further deepen our understanding on the energy exchange in the family of dark soliton and provide researchers a useful way on how to control and utilize dark soliton that might have impacts for future optical communication system.

References

[1] Y. S. Kivishar and G. Agrawal, *Optical Solitons: From Fiber to Photonic Crystals*. New York, NY, USA, Academic, 2003.
[2] Y. S. Kivshar and B. Luther-Davies, "Dark optical solitons: Physics and applications," *Phys. Rep.*, vol. 298, no. 2/3, pp. 81–197, May 1998.
[3] D. J. Frantzeskakis, "Dark solitons in atomic Bose-Einstein condensates: From theory to experiments," *J. Phys. A, Math. Theor.*, vol. 43, no. 21, May 2010, Art. ID. 213001.
[4] S. Burger, K. Bongs, S. Dettmer, W. Ertmer, and K. Sengstock, "Dark solitons in Bose-Einstein condensates," *Phys. Rev. Lett.*, vol. 83, no. 25, pp. 5198–5201, Dec. 1999.
[5] A. Muryshev, G. V. Shlyapnikov, W. Ertmer, K. Sengstock, and M. Lewenstein, "Dynamics of dark solitons in elongated Bose-Einstein condensates," *Phys. Rev. Lett.*, vol. 89, Aug. 2002, Art. ID. 110401.
[6] T. Tsuzuki, "Nonlinear waves in the Pitaevsldi-Gross equation," *J. Low Temp. Phys.*, vol. 4, no. 4, pp. 441–457, 1971.

[7] A. Hasegawa and F. Tappert, "Transmission of stationary nonlinear optical pulses in dispersive dielectric fibers—II. Normal dispersion," *Appl. Phys. Lett.*, vol. 23, no. 4, pp. 142–144, Aug. 1973.

[8] D. Krokel, N. J. Halas, G. Giuliani, and D. Grischkowsky, "Dark-pulse propagation in optical fibers," *Phys. Rev. Lett.*, vol. 60, no. 1, pp. 29–32, Jan. 1988.

[9] H. Zhang, D. Y. Tang, L. M. Zhao, and X. Wu, "Dark pulse emission of a fiber laser," *Phys. Rev. A*, vol. 80, Oct. 2009, Art. ID. 045803.

[10] M. Nakazawa and K. Suzuki, "10Gbit/s pseudorandom dark soliton data transmission over 1200 km," *Electron. Lett.*, vol. 31, no. 13, pp. 1076, Jun. 1995.

[11] C. R. Menyuk, "Stability of solitons in birefringent optical fibers—I: Equal propagation amplitudes," *Opt. Lett.*, vol. 12, no. 8, pp. 614–616, 1987.

[12] T. Ueda and W. L. Lath, "Dynamics of coupled solitons in nonlinear optical fiber," *Phys. Rev. A*, vol. 42, pp. 563–571, Jul. 1990.

[13] B. Crosignani and P. Di Porto, "Soliton propagation in multimode optical fibers," *Opt. Lett.*, vol. 6, no. 7, pp. 329–330, Jul. 1981.

[14] Q.-H. Park and H. J. Shin, "Systematic construction of vector solitons," *IEEE J. Sel. Topics Quantum Electron.*, vol. 8, no. 3, pp. 432–439, May/Jun. 2002.

[15] R. Gumenyuk, M. S. Gaponenko, K. V. Yumashev, A. A. Onushchenko, and O. G. Okhotnikov, "Vector soliton bunching in thulium-holmium fiber laser mode-locked with PbS quantum-dot-doped glass absorber," *IEEE J. Quantum Electron.*, vol. 48, no. 7, pp. 903–907, Jul. 2012.

[16] H. Zhang, D. Y. Tang, L. M. Zhao, and N. Xiang, "Coherent energy exchange between components of a vector soliton in fiber lasers," *Opt. Exp.*, vol. 16, no. 17, pp. 12618–12623, Aug. 2008.

[17] C. Anastassiou *et al.*, "Energy-exchange interactions between colliding vector solitons," *Phys. Rev. Lett.*, vol. 83, pp. 2332–2335, Sep. 1999.

[18] L. Salasnich and B. A. Malomed, "Vector solitons in nearly one-dimensional Bose-Einstein condensates," *Phys. Rev. A*, vol. 74, Nov. 2006, Art. ID. 053610.

[19] S. K. Adhikari, "Bright solitons in coupled defocusing NLS equation supported by coupling: Application to Bose-Einstein condensation," *Phys. Lett. A*, vol. 346, no. 1–3, pp. 179–185, Oct. 2005.

[20] Y. S. Kivshar and S. K. Turitsyn, "Vector dark solitons," *Opt. Lett.*, vol. 18, no. 5, pp. 337–339, Mar. 1993.

[21] A. P. Sheppard and Y. S. Kivshar, "Polarized dark solitons in isotropic Kerr media," *Phys. Rev. E*, vol. 55, pp. 4773–4782, Apr. 1997.

[22] E. Seve, G. Millot, and S. Wabnitz, "Buildup of terahertz vector dark-soliton trains from induced modulation instability in highly birefringent optical fiber," *Opt. Lett.*, vol. 23, no. 23, pp. 1829–1831, Dec. 1998.

[23] P. Öhberg and L. Santos, "Dark solitons in a two-component Bose-Einstein condensate," *Phys. Rev. Lett.*, vol. 86, no. 14, pp. 2918–2921, Apr. 2001.

[24] V. A. Brazhnyi and V. V. Konotop, "Stable and unstable vector dark solitons of coupled nonlinear Schrödinger equations: Application to two-component Bose-Einstein condensates," *Phys. Rev. E*, vol. 72, Aug. 2005, Art. ID. 026616.

[25] M. J. Ablowitz, T. P. Horikis, S. D. Nixon, and D. J. Frantzeskakis, "Dark solitons in mode-locked lasers," *Opt. Lett.*, vol. 36, no. 6, pp. 793–795, Mar. 2011.

[26] D. Tang *et al.*, "Dark soliton fiber lasers," *Opt. Exp.*, vol. 22, no. 16, pp. 19 831–19 837, Aug. 2014.

[27] D. Y. Tang, H. Zhang, L. M. Zhao, and X. Wu, "Observation of high-order polarization-locked vector solitons in a fiber laser," *Phys. Rev. Lett.*, vol. 101, Oct. 2008, Art. ID. 153904.

[28] N. G. Usechak and G. P. Agrawal, "Semi-analytic technique for analyzing mode-locked lasers," *Opt. Exp.*, vol. 13, no. 6, pp. 2075–2081, Mar. 2005.

[29] C. Jirauschek and F. Ö. Ilday, "Semianalytic theory of self-similar optical propagation and mode locking using a shape-adaptive model pulse," *Phys. Rev. A*, vol. 83, Jun. 2011, Art. ID. 063809.

[30] M. Sahaa, A. K. Sarma, and A. Biswas, "Dark optical solitons in power law media with time-dependent coefficients," *Phys. Lett. A*, vol. 373, no. 48, pp. 4438–4441, Dec. 2009.

[31] H. Triki and A. Biswas, "Dark solitons for a generalized nonlinear Schrödinger equation with parabolic law and dual-power law nonlinearities," *Math. Method. Appl. Sci.*, vol. 34, no. 8, pp. 958–962, 2011.

[32] A. Komarov, H. Leblond, and F. Sanchez, "Quintic complex Ginzburg-Landau model for ring fiber lasers", *Phys. Rev. E*, vol. 72, Aug. 2005, Art. ID. 025603.

[33] Z. Chen, M. Acks, E. A. Ostrovskaya, and Y. S. Kivshar, "Observation of bound states of interacting vector solitons," *Opt. Lett.*, vol. 25, no. 6, pp. 417–419, Mar. 2000.

[34] W. Zhao and E. Bourkoff, "Interactions between dark solitons," *Opt. Lett.*, vol. 14, no. 24, pp. 1371–1373, Dec. 1989.